RSC Advances

ROYAL SOCIETY OF CHEMISTRY

www.rsc.org/advances

Electronic structures and optical properties of TM (Cr, Mn, Fe or Co) atom doped ZnSe nanosheets

Xin-Lian Chen*, Bao-Jun Huang,Yong Feng, Pei-Ji Wang , Chang-Wen Zhang, Ping Li

Abstract: The electronic structures and optical properties of pristine and transition-metal（TM） atom doped ZnSe nanosheets (ZnSeNSs) have been studied based on first-principles calculations. The results indicate that the pristine ZnSeNSs are nonmagnetic direct gap semiconductors, while Mn, Fe or Co doped ZnSeNSs are all spin-polarized, and Cr doped one is half-metallic with 100% spin-polarized currents. Cr or Co doped ZnSeNSs can improve the absorption properties and broaden absorption range, compared to pristine, Fe or Mn doped ZnSeNSs. Moreover, the red-shift phenomena are observed. These results can provide an important reference for designing and fabricating infrared and visible photoelectric nanodevices.

Keywords: ZnSeNSs, first- principle calculations, electronic structures, optical properties

1. Introduction

More and more attentions have been paid to II-IV semiconductor compounds and their alloys due to their important applications in optoelectronic devices and detectors.[1] Zinc-selenide (ZnSe) is an II-IV compound semiconductor with band gap of 2.70eV at room temperature and has two well- known structural phases: zinc blend structure and wurtzite structure [2]. ZnSe is commonly used for CO_2 laser focusing lenses, night vision applications, ATR prisms and transmission windows for IR spectroscopy. In addition, because ZnSe doesn't contain toxic elements, as an environment friendly semiconductor material, it is widely used in the blue light emitting diodes (LED) and laser diodes [3-4].In the photocatalytic applications, ZnSe has been confirmed to be promising material to enhanced photocatalytic activities[5].

Recently, ZnSe nanostructures, such as thin films [6-7], nanobelts, nanorods [8], and nanoribbons[9-10] have been successfully synthesized in experiments by different

* *School of Physics and Technology, University of Jinan, Shandong, 250022, People's Republic of China*
E-mail：xinlianchen@163.com; *Tel: +86 531 82765976*

methods. Despite the synthesis of the large-scale ZnSe nanosheets (NSs) is very difficult, they have been reported to be successfully synthesized. Sun *et al.* [11] reported the ZnSeNSs with zinc blende structure synthesized by soft template method. H.Park *et al.* [12] synthesized the ZnSeNSs with zinc wurtzite structure by facile chemical method. Feng *et al.*[13] have constructed the large-scaled ZnSeNSs by ZnSe nanoparticles and showed that the ZnSeNSs were more suitable for the degradation of Rhodamine B under UV radiation, compared to ZnSe nanoparticles.

The nanosheets structures have many excellent properties because of its larger specific surface area and their unique quantum confinement effect. The better optical properties can be obtained in the nanosheets by doping elements. The electronic structure and optical properties of the nanosheets doped have been reported by a body of works, such as transition-metal (TM) doped SnO_2 NSs[14], Ag-doped SnO2 monolayer [15], and C, V or In-doped ZnO[16]. Many investigations and calculations have been performed about the structural, electronic, and optical properties of the bulk ZnSe materials[17-19]. Cr and Fe doped ZnSe have been used to laser gain medium in mid-IR laser[20-21]. So far, few works theoretically reported the electronic structure and optical properties of ZnSeNSs, especially, TM atom doped ZnSeNSs.

In this work, we performed first-principle spin polarized calculation to study the electronic structures and optical properties of TM doped ZnSeNSs. Zn atom was replaced by TM (Cr, Mn, Fe or Co) atom in ZnSeNSs. Firstly, the defect formation energy is calculated to determine the stability of TM-doped ZnSeNSs. Secondly, we studied the electronic properties of TM (Cr, Mn, Fe or Co) atom doped ZnSeNSs. Thirdly, the optical properties of TM (Cr, Mn, Fe or Co) atom doped ZnSeNSs are studied by analyzing the optical transitions between occupied and unoccupied states.

2. Method and calculation details

All the calculations were carried out by the WIEN2k based on the first-principles density function theory (DFT), which implements full potential linearized augmented plane wave (FLAPW) method [22]. To describe the exchange and correlation functional, the electronic and optical properties were calculated using a generalized gradient

approximation (GGA) proposed by Perdew–Bueke–Ernzerhof (PBE) [23]. The lattice parameters and atom position were optimized in order to determine structural stability of TM (Cr, Mn, Fe or Co) doped ZnSeNSs. And the k-point meshes for Brillouin zone were set as a 6×6×1 Monkhorst-Pack grids. The muffin-tin radii are chosen as 2.0 a.u. for Zn, Se, and TM (Cr, Mn,Fe or Co) atom. An energy cutoff of −7.0 Ry is employed for the LAPW basis to describe the wave functions in the interstitial region. The structural relaxation is done until the forces on each atom are smaller than10^{-4} eV/Å. A vacuum region of 10Å was applied along the direction perpendicular to the ZnSeNSs surface to achieve convergence on the parameters.

The pristine ZnSeNSs were selected with a 4×4×1 super cell cut from ideal bulk ZnSe with wurtzite structure, as shown in Fig.1. From Fig.1 (a)-(b), it is found that the optimized pristine ZnSeNSs forms graphene-like structure as seen from the side view, similar to ZnO NSs[24] and ZnS NSs [25]. The optimized lattice parameter is 4.096 Å and the length of Zn-Se bond is 2.38 Å, which are consistent with the experimental results[12]. Fig.1 (c) and (d) show the band structures and the density of states (DOS) of pristine ZnSeNSs, respectively. From Fig.1(c), the pristine ZnSeNSs is a direct gap semiconductor with the band gap of about 1.85eV because the conduction band minimum (CBM) and the valence band maximum (VBM) are located at the Γ point in the Brillouin zone. In fact, the calculated band gap is smaller than experimental value because of underestimating the correlation interaction between excited electrons in the calculation [26]. Compared to the bulk ZnSe (~1.35eV), the band gap of pristine ZnSeZNSs increased, similar to the case of ZnONSs[27, 28]. In addition, the pristine ZnSeNSs is nonmagnetic due to a symmetrical distribution of the wave functions of spin-up and spin-down channels, and the spin-up DOS is shown in Fig.1 (d).

In the following study, we perform the effect of TM atom (Cr, Mn, Fe or Co) substitution for Zn atom in ZnSeNSs. The position of the doping atom is located at blue ball position in Fig.1 (a). And the calculated results are compared to those of pristine ZnSeNSs.

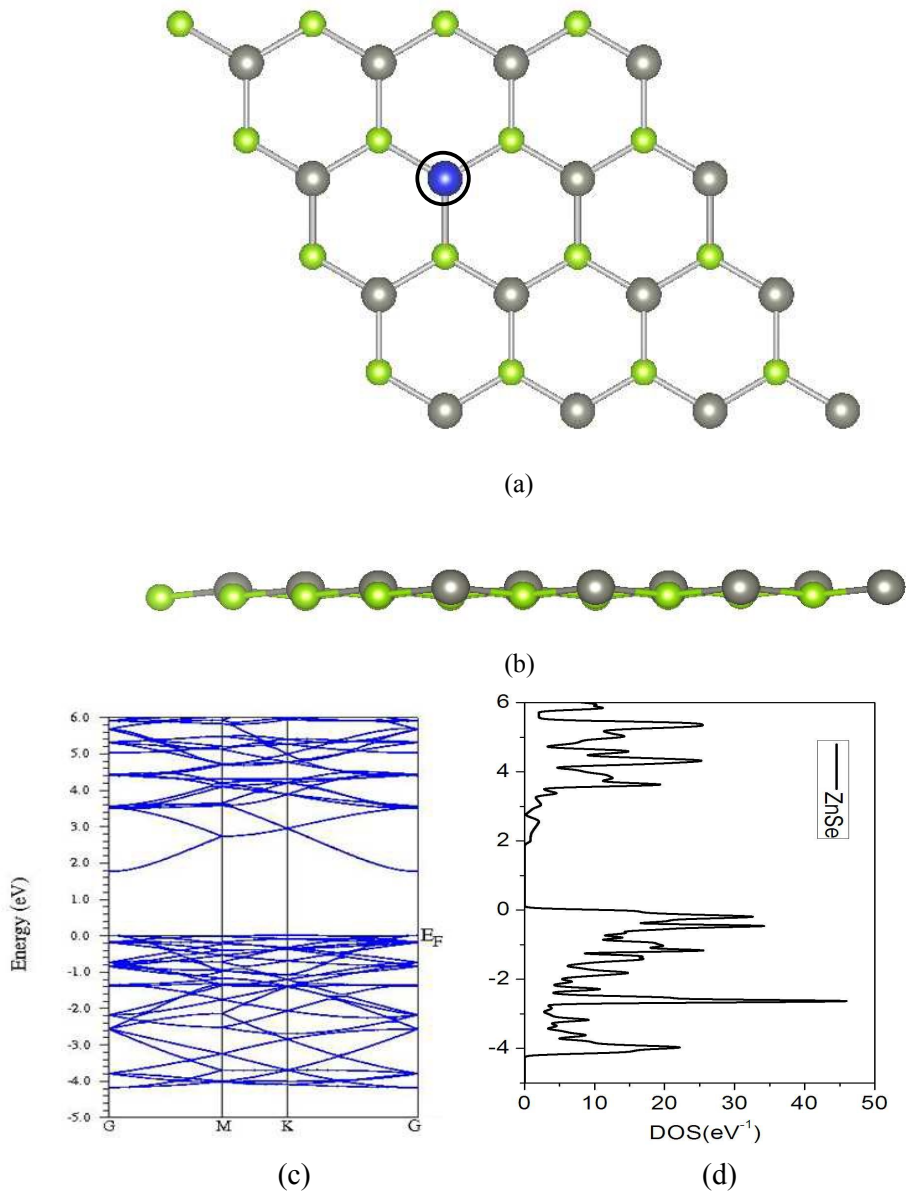

Fig. 1 (a) Top view of pristine ZnSeNSs (the position of Zn is denoted by blue ball in the circle) (b) side view of pristine ZnSeNSs (c) the band structure of pristine ZnSeNSs (d) DOS of pristine ZnSeNSs (spin up)

3. Results and discussion

3.1 Formation energy

The stability of TM-doped ZnSeNSs can be determined by the defect formation energy (E_f), defined as $E_f = E_{X:ZnSe} - E_{ZnSe} + u_{Zn} - u_x$ [29], where $E_{X:ZnSe}$ and E_{ZnSe} are

the total energies of the TM-doped ZnSeNSs and ZnSeNSs supercell, respectively. u_{Zn} is the chemical potentials of Zn and u_x is those of TM atom(Cr, Mn, Fe, or Co). The smaller the value of E_f, the structure is more stable. The values of E_f are shown in Table I. From the Table I, the TM (Cr, Mn, Fe or Co) atom doped ZnSeNSs all release energy. This indicates that Cr, Mn, Fe or Co as a dopant can achieve a more stable structure than pristine ZnSeNSs. Moreover, for optimized structures of TM (Cr, Mn, Fe or Co) atom doped ZnSeNSs, it is found that the bond length between doped TM atom and its nearest Se atom ($d_{x\text{-}Se}$) has changed. The atom radius and electronegativity are mainly responsible for the bond length change. The bond length of Fe or Co and Se bond is less than Zn-Se bond because of Zn atom substituted by smaller ionic radius of Fe or Co. And for Cr or Mn doped ZnSeNSs, the opposite happens because Cr or Mn has less electronegativity than Zn atom. In addition, we find that TM (Cr, Fe, Mn or Co) atom doped ZnSeNSs show magnetic properties, which the total magnetic moments per Cr, Fe, Mn, and Co dopant are 4.89, 5.92, 4.89, and 3.87 μ_B, respectively. This mainly came from the strong localized magnetic moment caused by the doped atoms[14].Take Cr doped ZnSeNSs for example, when Cr atom substituted for Zn atom, one 4s electron and one 3d electron of Cr atom transition to the 4p orbit of Se atom, thus the 4p orbit of Se is completely stained. Four spin-up electrons still exists in the 3d orbit of Cr and the magnetic moment is given by $M = g\sqrt{s(s+1)}\mu_B = 2*\sqrt{2*(2+1)}*\mu_B = 4.89\mu_B$ .Here, [ ] and [ ] are Landé factor and the half of the unpaired electrons, respectively.

Table I: The bond length between TM atom and its nearest Se atom ($d_{x\text{-}Se}$), the defect formation energy (E_f) whose "-" represents the releasing energy, the number of unpaired electrons (N) and the total magnetic moment (M).

Configurations	$d_{x\text{-}Se}$ (Å)	E_f(eV)	*N*	$M(\mu_B)$
ZnSe	2.376	--	0	0
Cr:ZnSe	2.486	-1.93	4.0	4.89
Mn:ZnSe	2.415	-2.05	5.0	5.92
Fe:ZnSe	2.366	-2.21	4.0	4.89
Co:ZnSe	2.358	-2.64	3.0	3.87

3.2 Band structure and density of electronic states

The spin band structures for TM (Cr, Mn, Fe or Co) atom doped ZnSeNSs are illustrated in Fig. 2 (a)-(d), respectively. We can find that the spin band structures of TM atom doped ZnSeNSs become more complicated than those of pristine ZnSeNSs due to the emergence of the impurity energy levels. From Fig.2, several obvious features can be obtained. Firstly, TM (Cr, Mn, Fe or Co) atom doped ZnSeNSs still remain direct band gap character with the same as pristine ZnSeNSs. Secondly, TM (Cr, Mn, Fe or Co) atom doped ZnSeNSs are all spin-polarized due to the asymmetrical distribution of band structures of spin-up and spin-down channels. From Fig. 2(a), Cr-doped ZnSeNSs show half-metallic with 100% spin-polarized currents. This can be caused by the hybridization both Cr 3d and Se 4p states near the Fermi level. However, Mn, Fe or Co doped ZnSeNSs have the similar characteristics by analyzing the spin band structures. They are all the semiconductors, but some impurity energy levels can be found near the Fermi level, which mainly come from the 3d states of the TM doped atom and 4p states of the Se atom. The appearance of the impurity energy levels with more active electronic transition from the occupied bands to unoccupied bands may be good for improving the optical properties.

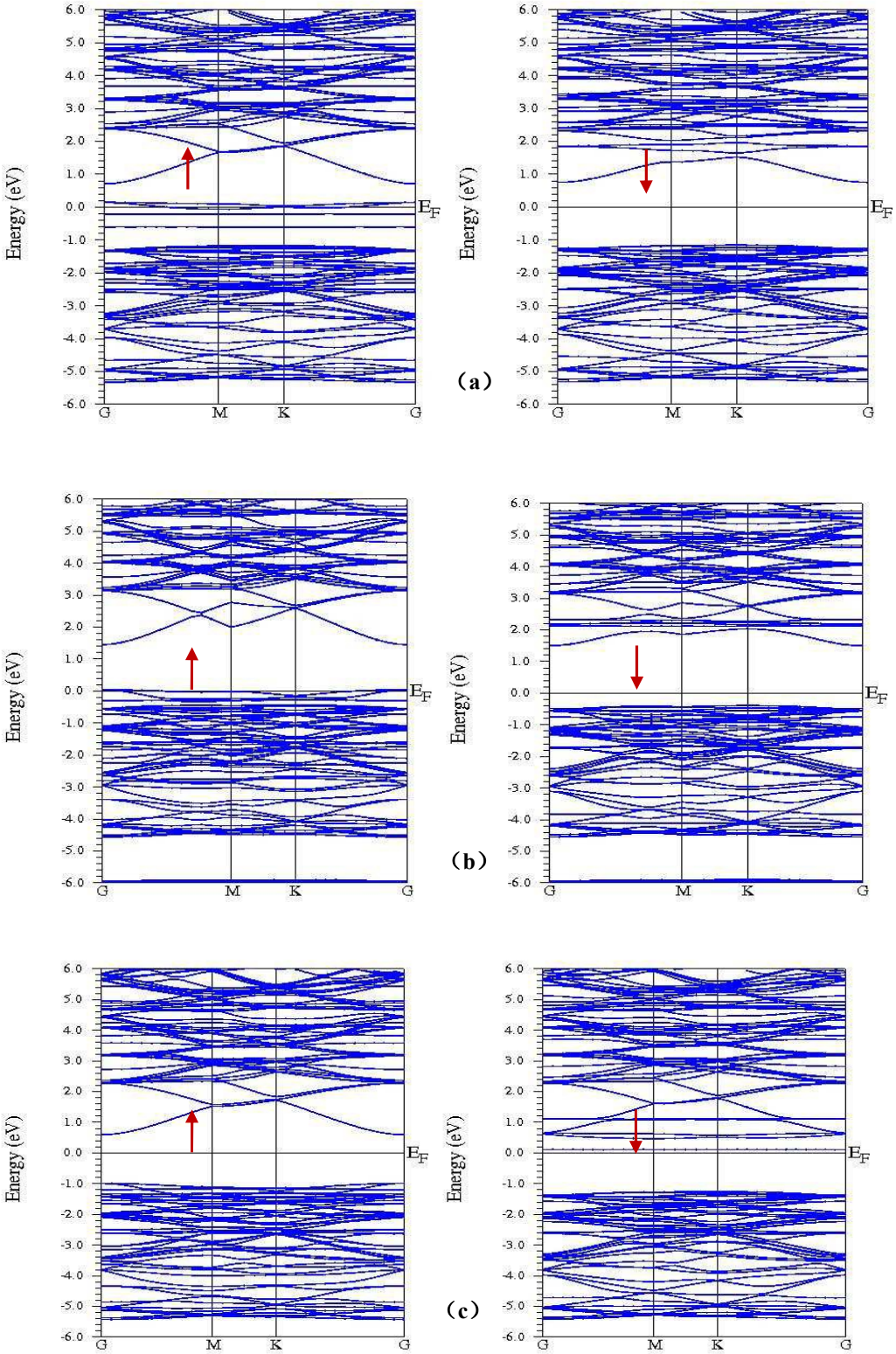

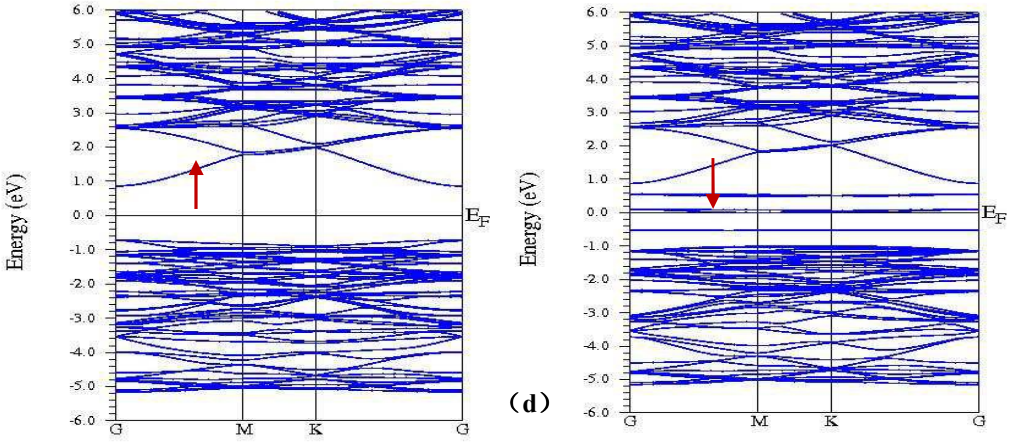

Fig.2 the spin band structures for TM atom (Cr, Mn, Fe or Co) doped ZnSeNSs (a) Cr, (b) Mn, (c) Fe, and (d) Co atom. The arrows "↑" and "↓" represent spin-up and spin-down, respectively.

To further analyze the effect of TM (Cr, Fe, Mn or Co) doping on the electronic and optical properties of ZnSeNSs, we calculated the total density of states (TDOS) and partial density of states (PDOS) of TM-doped ZnSeNSs, as shown in Fig. 3. The results show that Cr doped ZnSeNSs exhibits magnetic half-metal properties, while Mn, Fe, or Co doped ZnSeNSs are all magnetic semiconductors. Moreover, for Cr or Co doped ZnSeNSs in Fig.3 (a) and Fig.3(d), the electronic states near the Fermi level mainly consists of doped atom 3d states strongly hybridized with Se 4p states, while Zn 4s states plays a major role to form the conductive band. The band gap reduction and the red-shift phenomenon are also found. From Fig.3 (b), the valence band of Mn doped ZnSeNSs is mainly supplied by Mn 4s states and Se 4p while the conduction band is supplied by Mn 4s and Zn 4s states. From Fig.3(c), the valence band of Fe doped ZnSeNSs is mainly caused by the hybridization of Fe 3d states and Se 4p states, while the conduction band near the Fermi level is caused by Fe 3d states.

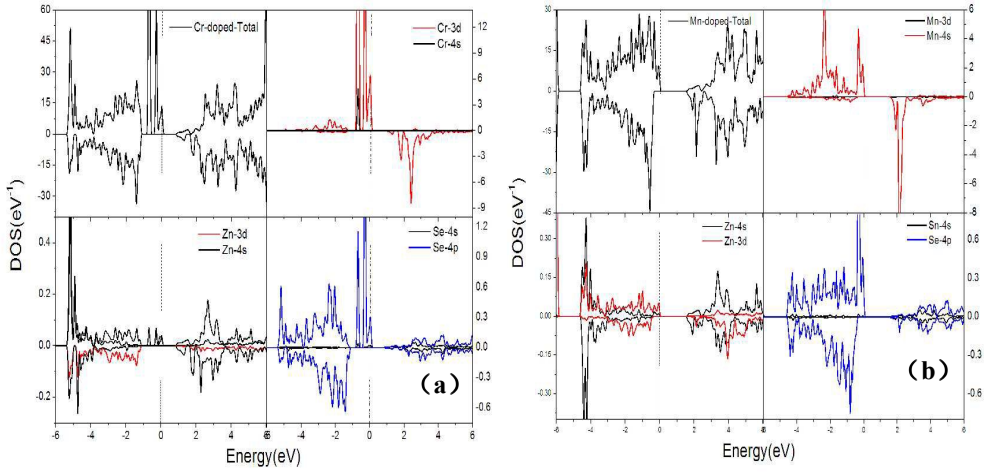

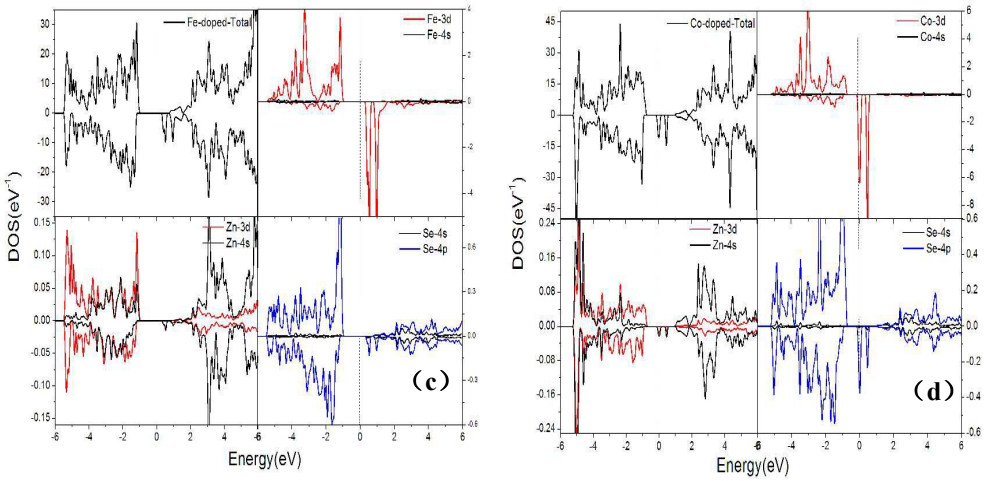

Fig.3 Total and partial DOS for (a) Cr, (b) Mn, (c) Fe, and (d) Co atom and nearest Zn, Se atoms. Fermi level E_F is set to zero and the vertical dashed lines denote E_F.

Usually, the GGA method can underestimate the binding energy of d states. In order to check our results, we calculated the TM atom 3d orbit by GGA+U (U=3.0eV) and the results are shown in Fig.4.Fig.4 shows the total DOS of TM-doped ZnSeNSs and partial DOS of 3d atom. Compared with GGA results, the amount of impurity energy level becomes less around the Fermi energy and the band gap is larger. This shows that GGA underestimates that the TM atom 3d orbitals hybridization quite strongly with Se 4p orbitals. Furthermore, we found the same results for the magnetic moments can be derived by the GGA+U and GGA method. Comparison results show that the results by the GGA method can qualitatively reflect the properties of TM atom doped ZnSeNSs. Compared with TM atom doped SnO_2 [14], similar results can be derived.

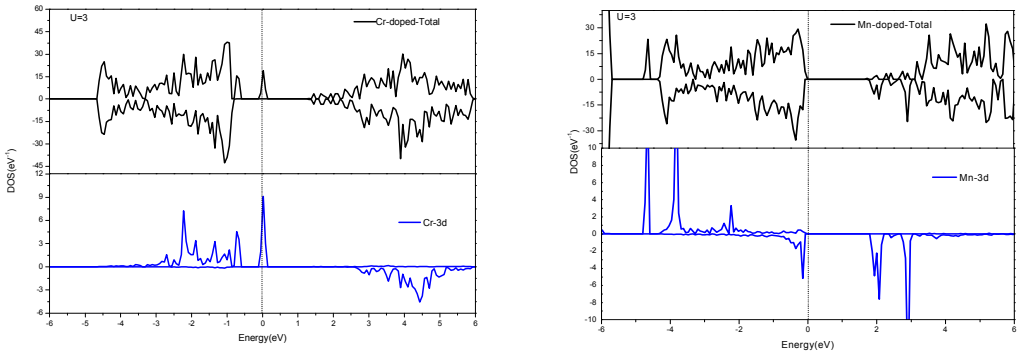

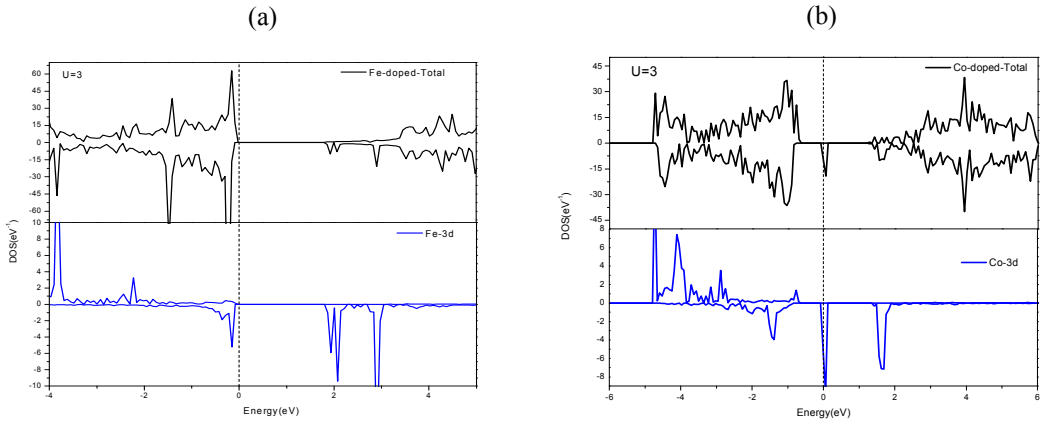

Fig.4 Total and TM atom 3d partial DOS with U=3. (a) Cr, (b) Mn, (c) Fe, and (d) Co. Fermi level is set to zero. DOS is broadened by Gaussian smearing with 0.2 eV.

3.3 Optical properties

In our work, the optical properties of TM (Cr, Mn, Fe or Co) doped ZnSeNSs have also been studied. It is helpful to study the optical properties of the medium by analyzing the optical transitions between occupied and unoccupied states. The imaginary part of the dielectric tensor can be computed from the electronic band structure of solid. The optical properties can be obtained from the complex dielectric function. It can be expressed as [30-31]

$$\varepsilon(\omega) = \varepsilon_1(\omega) + i\varepsilon_2(\omega) \tag{1}$$

The real part of the dielectric function $\varepsilon_1(\omega)$ can be evaluated from the imaginary part $\varepsilon_2(\omega)$ via the Kramers–Kronig transform. And according to Ref.32, the imaginary part of the dielectric function $\varepsilon_2(\omega)$can be expressed as

$$\varepsilon_2(\omega) = \frac{4\pi^2}{m^2\omega^2}\sum_{V,C}\int_{BZ} d^3k \frac{2}{2\pi}\left|e\cdot M_{cv}(K)\right|^2 \times \delta[E_C(k) - E_V(k) - \hbar\omega] \tag{2}$$

Here, C, V, and BZ represent conduction band, valence band, and the first Brillouin zone, respectively. k is reciprocal lattice vector and ω is angular frequency. $E_C(k)$ and $E_V(k)$ are pristine energy level of conduction band and valence band, respectively. $|M_{cv}(K)|^2$ is momentum matrix element. The imaginary parts of the dielectric function for pristine and TM atom doped ZnSeNSs are shown in Fig.5.

From Fig.5, the imaginary parts of the dielectric functions for TM (Cr, Mn, Fe or Co) doped ZnSeNSs are larger than pristine ZnSeNSs. In low energy region, there are obvious increments for Co and Cr doped ZnSeNSs. This can be explained by the emergence of some impurity energy levels around the Fermi level and the larger probability of the electron transition. For Co doped ZnSeNSs, there are two peaks in the low energy region. The reason can be mainly attributed to the transition between Se 4p states in the top of valence band and Co 3d states in the conduction band near the Femi level. For Cr doped ZnSeNSs, an obvious peak appears around the 1.4eV, which derived from the transition between Cr 3d and Se 4p states. However，a small peak originated from the transition between the energy levels in the top of the valence band and the bottom of the conduction band is observed around 0.4eV for Fe doped ZnSeNSs. For Mn doped ZnSeNSs in the region of less than 1.6eV, the imaginary part of dielectric function approaches to zero, similar to the pristine ZnSeNSs. The imaginary part of dielectric function with TM doped ZnSeNSs has larger increase around 4.5eV compared with the pristine ZnSeNSs. It is mainly due to the inter-band transition between the valence band and the conduction band.

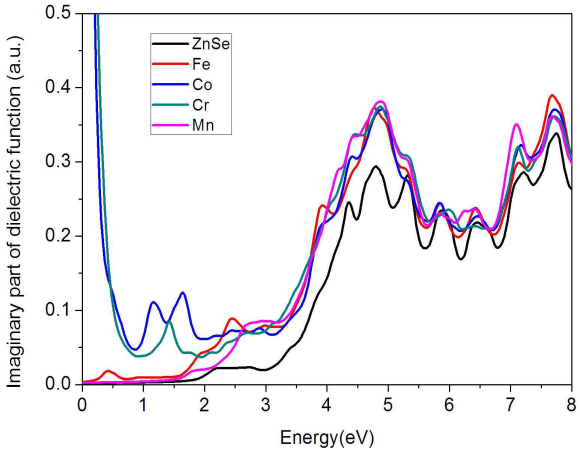

Fig.5 (Color online) The imaginary part of dielectric functions of TM doped ZnSeNSs

The absorption property of the semiconductor is related to its electronic band structure. The absorption coefficient can be expressed as

$$I(\omega) = \sqrt{2}\omega\left[\sqrt{\varepsilon_1^{\,2}(\omega) - \varepsilon_2^{\,2}(\omega)} - \varepsilon_1(\omega)\right]^{1/2} \quad (3)$$

The absorption coefficients for TM (Cr, Mn, Fe or Co) doped ZnSeNSs are illustrated in Fig.6. From Fig.6, it can be found that the positions of absorption peaks of pristine ZnSeNSs were significantly blue-shifted from those of bulk ZnSe (E_g=2.7-2.8eV), which are consistent with the experimental results[33].The absorption coefficient of TM doped ZnSeNSs above the fundamental absorption edges becomes stronger than that of the pristine ZnSeNSs, which is more suitable to make the photoelectric device. Compared to the pristine ZnSeNSs, the red-shift is observed for Cr or Co doped ZnSeNSs and the absorption coefficient is near zero for Mn or Fe below absorption edges. This phenomenon can be caused by the impurity energy level around the Fermi level. The results show that Cr or Co doped ZnSeNSs have better optical properties and broaden the absorption range, compared to Fe or Mn doped ZnSeNSs. They can be widely used in infrared and visible photoelectric devices.

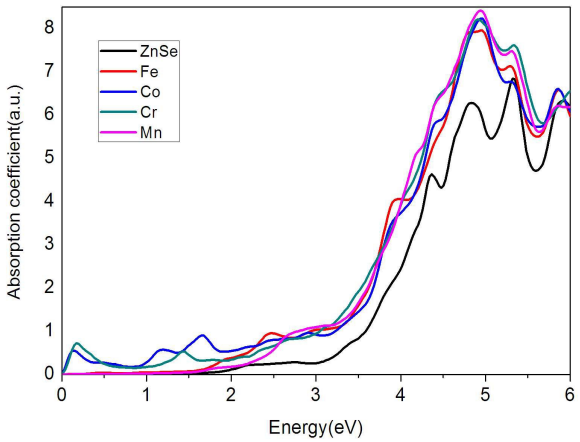

Fig.6 (Color online) The absorption coefficients of TM doped ZnSeNSs.

4. Conclusion

In this paper**,** we have presented the theoretical calculations for the electronic structures and optical properties of TM (Cr, Mn, Fe or Co) ZnSeNSs based on first-principles density function theory (DFT), which implements full potential linearized augmented plane wave (FLAPW) method. The results show that Fe, Mn or Co atom doped ZnSeNSs possess direct band gap semiconductor with magnetic property , while Cr atom doped ZnSeNSs is half-metallic with 100% spin-polarized currents. Furthermore, the imaginary part of dielectric function and absorption coefficient are increased significantly in the visible region. Simultaneously, the

ZnSeNSs with Cr or Co doping have better optical properties in infrared region and the red-shift phenomenon happens because the absorption edge shifts to the low energy region compared to pristine, Fe or Mn doped ZnSeNSs.. These results provide some theoretical basics for the further design and application in infrared and visible photoelectric devices.

5. Acknowledgements

This work was supported by the National Natural Science Foundation of China (Grant No. 11274143, 61172028), The National Natural Science Foundation of Shandong Province(Grant No.ZR2013AL004, ZR2013AL002), Technological Development Program in Shandong Province Education Department (J14LJ03), Research Fund for the Doctoral Program of University of Jinan (Grant no. XBS1433, XBS1402, and XBS1452).

References

1 B. I. Adetunji, P. O. Adebambo, G.A..Adebayo. *J. Alloys Compd*, 2012, **513,** 294-299.
2 J.A. Liu, X.L.Wei, Y.Qu, J.H.Cao, C.S.Chen, H.Jiang. Mater Lett, 2011, **65**, 2139–2141.
3 M. A. Haase, J. Qiu, J. M. DePuydt, and H. Cheng, Blue-green laser diodes, *Appl. Phys. Lett.* , 1991, **59**, 1271.
4 D. B. Eason, Z. Yu, W. C. Hughes, W. H. Roland, C. Boney, J. W. Cook, J. F. Schetzina, G. Cantwell, W. C. Harsch, Appl. Phys. Lett. , 1995, **66**, 115.
5 J.L. Xu, W.Wang, X.Zhang, X.J.Chang, Z.N Shi, G. M. Haarbergc.. *J. Alloys Compd,* 2015, **632**,778-782.
6 U. Khairnar, S. Behere and P. Pawar, *Material Sciences and Applications,* 2012, 3, 36-40
7 T.M. Khan , M. F. Mehmood, A. Mahmood,A. Shah, Q. Raza,Amjid Iqbal, U. Aziz. *Thin Solid Films* , 2011,519, 5971–5977.
8 Q.Z. Zeng, S.L. Xue, S.X. Wu, K.X. Gan, L. Xu, J.W. Han, W.K. Zhou, Y.T. Shi, R.J. Zou, *Materials Science in Semiconductor Processing*, 2015, **31**, 189–194
9 X.W. Zhang, X.J. Zhang, X.Z. Zhang, Y.P. Zhang, L. Bian, Y.M. Wu, C. Xie, Y.Y. Han, Y.Wang, P. Gao, L. Wang and J.S. Jie. *J. Mater. Chem.,* 2012, **22**, 22873-22880.
10 Y.Q.Zou, H.L.Li, P.Y.Ren, J.Y.Xu, L. Ma, X.X. Wang, X.P. Fan, Z.P. Shan, X.J. Zhuang, H. Zhou, X.L. Zhu, Q.L. Zhang, A.L. Pan, *Materials Letters*, 2014,**129,** 118–121.
11 Y.F. Sun, Z.H. Sun, S. Gao, H .Cheng, Q.H. Liu, J.Y Pia, *Nat. Commun.,* 2012, **3, 1057**.
12 H. Park, H. Chung, W. Kim, *Materials Letters,* 2013, **99**,172–175.
13 B. Feng, J.H. Yang, J. Cao, L.L.Yang, M. Gao, M.B. Wei, H.J. Zhai, Y.F. Sun, *J. Alloys Compd*, 2013,**555**, 241–245
14 Y. Feng, W.X. Ji, B.J. Huang, X.L Chen, F. Li, P. Li, C.W. Zhang, P.J. Wang. T, *RSC Adv.,* 2015, **5**, 24306
15 B.J. Huang, F. Li, C.W. Zhang, P. Li. P.J. Wang. *RSC Adv.*, 2014, **4**, 41819

16 F.B. Zheng, C.W. Zhang, P.J. Wang, H. X. Luan, *J. Appl. Phys.* ,2012,**111**, 044329 .

17 S. Zh. Karazhanov, P. Ravindran, A. Kjekshus, H. Fjellvåg, and B. G. Svensson, *Phys. Rev. B* , 2007,**75**, 155104

18 P.K. SAINI, D. SINGH, D.S. AHLAWAT, Chalcogenide Letters, 2014, **11**(9), 405 – 414.

19 R. Khenata , A. Bouhemadou, M. Sahnoun, Ali. H. Reshak, H. Baltache, M. Rabah., *Computational Materials Science*, 2006, **38**, 29–38

20 S. B. Mirov, V. Fedorov, D. Martyshkin, I. Moskalev, M. Mirov, and V. Gapontsev, "Progress in Cr and Fe Doped ZnSe and ZnS Polycrystalline Materials and Lasers," *Advanced Solid State Lasers*, 2014, **AM4A.6**, 16-21

21 N. Myoung, M. S. Mirov, V. V. Fedorov, S. B. Mirov, *Laser Applications to Photonic Applications*, 2011, **CMY4**,1-6

22 K. Schwarz, P. Blaha, G. Madsen, *Comp. Phys. Commun*. 2002,**147**, 71-76.

23 J. P. Perdew, K. Burke, M. Ernzerhof, *Phys. Rev. Lett. ,* 1996, *77*, 3865.

24 L.L. Yang, Z. Wang, Z.Q. Zhang, Y. F. Sun, M, Gao, J, H Yang, Y, S, Yan, *J. Appl. Phys.,* 2013, **113**, 033514

25 X.J. Zhang, M. W. Zhao, S. S. Yan, T. He, W. F. Li, X. H. Lin, Z. X. Xi, Z. H. Wang, X. D. Liu, Y. Y. Xia , *Nanotechnology*, 2008, 19, 305708

27 S.J. Pearton, D. P. Norton, K .Ip, Y. W. Heo, T. Steiner. *Progress in Materials Science*,2005, **50**, 293–340

28 X.Y.Feng, Z.Wang, C.W. Zhang,P.J.Wang, *Physica E,*2013, **54**,144–148

29 A. F. Kohan, G. Ceder, D. Morgan , C. G. Van de Walle, *Phys. Rev. B: Condens. Matter Mater. Phys.* 2000, **61**, 15019.

30 F. Wooten, Optical Properties of Solids .*Academic Press: New York*, 1972, ch.2, P152.

31 P.K. SAINIa, D. SINGHb, D.S. AHLAWATa, *Chalcogenide Letter*s, 2014, **11**, 405 - 414.

32 M. Naeem, S. K. Hasanain, A. Mumtaz, *J. Phys.: Condens. Matter. ,* 2008, **20**, 025210.

33 L. N. Liu , H.W. Song, L.B. Fan, F.Wang, R.F.Qin, B. Z. Dong, H.F.Zhao, X.G. Ren, G.H. Pan, X.Bai ,Q. L. Da. *Material Research Bulletin*, 2009,**44**, 1385–1391